SF2A 2012
S. Boissier, P. de Laverny, N. Nardetto, R. Samadi, D. Valls-Gabaud and H. Wozniak (eds)

MORPHOLOGY OF GALAXY CLUSTERS IN LARGE OPTICAL GALAXY SURVEYS

F. Rostagni[1], C. Benoist[1] and S. Maurogordato[1]

Abstract. We present a quantitative morphological classification of a sample of low redshift galaxy clusters extracted from the SDSS C4 cluster catalogue. Based on a wavelet analysis of both the galaxy velocity distribution and projected distribution, four morphological classes have been defined: regular, major multimodal, minor multimodal and irregular unimodal clusters. The method is applied to a subsample of 224 C4 clusters: 79 clusters (35%) are classified as regular, 51 (23%) as major multimodal, 16 (7%) as minor multimodal and 78 (35%) as irregular unimodal clusters.

Keywords: Galaxies: clusters: general, large scale structure of Universe

1 Introduction

Galaxy clusters are the largest gravitationally bound systems of the universe. According to the standard model of cosmology they formed recently through a hierarchical growth in which smaller units, galaxies and groups of galaxies, assemble together. Numerous observations in X-rays (Jones & Forman 1999) as well as in optical (Geller & Beers 1982; Dressler & Shectman 1988) show that there are substructures in a non negligible fraction of clusters, suggesting that clusters are currently in a non relaxed dynamical state. These results show that when using large cluster samples for statistical studies it is of prime importance to characterize systematically clusters' structural properties. Neglecting that a significant fraction of clusters can be far from relaxation could indeed bias severely any statement on the evolution of clusters or some of their scaling relations. It could in particular affect artificially the scatter of the mass-richness relation that is central to the use of cluster counts for constraining cosmological scenarios. In order to fully address the dynamical state of a cluster, one needs to trace both the gas and galaxies. In the present work we focus on the optical morphology.

Several works were performed in order to establish cluster morphological classifications. First, the cluster galaxy content was used to classify clusters (Bautz & Morgan 1970; Rood & Sastry 1971). In the eighties, with the advent of the X-ray astronomy, several powerful statistical tools were developed to analyze the cluster X-ray morphology. Mohr et al. (1993) used the centroid shift to constrain the dynamical state of 5 clusters observed with the *Einstein Observatory*. This technique was also used on more clusters (Jones & Forman 1999; Schuecker et al. 2001). Buote & Tsai (1996) developed the power ratio method, consisting in measuring the ratio between statistical moments of cluster X-ray luminosity. Cluster ellipticity was also used to assess cluster dynamical state (Kolokotronis et al. 2001; Melott et al. 2001; Plionis 2002).

Thanks to the development of multi-object spectroscopy, large redshift surveys were completed enabling to disentangle piled up structures along the line of sight. Numerous statistical tools were developed to evaluate cluster properties along the line of sight (Beers et al. 1990) and to check the Gaussianity of their redshift distribution (Ashman et al. 1994). In parallel, analyses of galaxy projected distribution were performed to detect substructures. Such studies were based on, for instance, adaptive kernels (Ramella et al. 2007) or wavelet analysis (Ferrari et al. 2005; Flin & Krywult 2006).

The aim of the present analysis is to establish a new optical cluster classification. In this analysis, galaxy positions and redshifts are used to characterize cluster optical morphology on a large homogeneous sample of nearby clusters: the C4 clusters catalog extracted from the SDSS, whose median redshift is 0.08. The classification method and the morphology indicators are explained in section 3 and the application to the sample is described in section 4.

In this paper, physical distances are computed assuming a flat universe with $H_0 = 70\mathrm{km.s}^{-1}$, $\Omega_M = 0.3$ and $\Omega_\Lambda = 0.7$.

[1] Laboratoire Lagrange, OCA, CNRS, UNS, boulevard de l'Observatoire 06304 Nice Cedex, France

2 Data description

Currently the Sloan Digital Sky Survey (York et al. 2000) is the sky survey best suited for analyzing the local universe. Miller et al. (2005) developed the C4 cluster finder algorithm and detected 749 clusters in SDSS DR2 (Abazajian et al. 2004). C4 clusters are the baseline of the present analysis. Photometric and spectroscopic information of all galaxies falling within 5Mpc from C4 cluster centers have been extracted into regions named *C4 fields* in the following. To assure a high degree of spectroscopic completeness, galaxies were selected to be brighter than $r = 17.77$. However, for geometrical reasons, the densest fields, that correspond to galaxy clusters, were not achieved with the same nominal completeness rate. To trace clusters and their potential substructures with enough accuracy, only fields with (i) a completeness larger than 50% and (ii) a central cluster core containing enough galaxies are kept. These two criteria plus the removal of clusters close to SDSS edges reduced the cluster sample from 749 to 237 clusters. Cluster coordinates (α, δ, z) were refined and only the main cluster among clusters closer than 2Mpc from each other was kept, leading to a final sample of 224 clusters. Clusters of this sample have redshifts ranging from 0.03 to 0.14, the median being 0.08, and velocity dispersions between 150 and 2500km.s^{-1}.

3 Morphological classification

In the present study, four categories of galaxy clusters are defined: regular, major multimodal, minor multimodal and irregular unimodal clusters. Regular clusters are defined as clusters having a Gaussian velocity distribution and characterized by an unique structure in projection on the plane of the sky with a spherical profile. Major multimodal clusters are defined as clusters presenting at least two close components with mass ratio greater than 1:5; minor multimodal clusters as clusters having one or more close components with mass ratio smaller than 1:5 and irregular unimodal clusters as clusters with one non Gaussian peak and/or one elliptical isolated clump.

Along the line of sight, the velocity distribution of clusters is fitted by a Gaussian mixture to search for multimodality and normality tests are performed. In projection, density maps are computed based on a multi-scale approach (see Ferrari et al. 2005, for a detailed description) and considering the scales corresponding to the typical cluster sizes: from 0.5Mpc to 2Mpc. Overdensities are then extracted from the image, their position (α, δ) and their properties (ellipticity and richness) are measured. Here, the multimodality is defined by the presence of overdensities within 2Mpc from the cluster. The type of multimodality is then defined by the richness ratio: overdensities with richness greater than a fifth of the one of the cluster are considered as major multimodals, while others are minor multimodals. The ellipticity of the main cluster is also used to classify isolated clusters: the ellipticity threshold was set to 0.3 to separate regular clusters ($\epsilon \leq 0.3$) from irregular unimodal clusters ($\epsilon > 0.3$).

4 Application to C4 clusters

In this section, the classification is applied to the subsample of 224 C4 clusters with the properties described in section 2. For each cluster, we defined a redshift range in order to optimize the selection of cluster members while minimizing contamination by interlopers. The cluster redshift distribution function (hereafter RDF) is computed using again a multi-scale approach in an aperture corresponding to an angular size of 1Mpc at the cluster C4 redshift. The cluster redshift is defined as the RDF mode and the redshift range is defined as the region in which the RDF is greater than 5% of its maximum value. Examples of RDFs are shown in left panels of fig. 1, with the C4 cluster redshift indicated in red and the redshift range in green.

After selecting galaxies within this redshift range, the redshift distribution is fitted by a Gaussian mixture and normality tests are performed. The decomposition into a Gaussian mixture is performed with EMMIX software (McLachlan & Peel 1999) and the normality tests with ROSTAT software (Beers et al. 1990). Furthermore to assess the quality of fits, the χ^2 was computed between the best fit (ROSTAT fit for single Gaussian peak clusters and EMMIX fit for the others) and the RDF computed with the wavelet analysis. The value of 0.2 is chosen to separate Gaussian $\left(\chi^2 \leq 0.2\right)$ from non Gaussian distributions $\left(\chi^2 > 0.2\right)$.

In order to study the projected distribution of galaxies, density maps have been computed as described in section 3 using all galaxies of the whole *C4 field* and within the previously defined redshift range. SExtractor software (Bertin & Arnouts 1996) was used to detect overdensities in the density maps. The flux measured by SExtractor corresponds to a richness, *i.e.* the number of galaxies in an overdensity with $r \leq 17.77$. For the present analysis, only overdensities with richness greater than 5 are kept as relevant. Physical projected distances (at the cluster redshift) are computed between overdensities and the main cluster (at the center) and richness ratios are computed. Examples of density maps are shown in right panels of fig. 1 with the detected overdensities (red ellipses) and the 2Mpc radius represented by the green circle around the main cluster.

Finally, the 224 clusters have been classified into the four morphological categories previously defined: 79 clusters (35%) are classified as regular clusters, 51 (23%) as major multimodal clusters with mass ratio greater than 1:5, 16 clusters (7%) as minor multimodal clusters with mass ratio smaller than 1:5 and the remaining 78 clusters (35%) as irregular unimodal clusters, without substructure. An example of each class is shown in figure 1. The C4 cluster 0007 (top panels of fig. 1) is a regular cluster: its velocity distribution is Gaussian with $\chi^2 = 0.045$, it has no neighbour within 2Mpc and it has a small ellipticity $\epsilon = 0.19$. On the second line of figure 1, the C4 cluster 0082 is a major multimodal cluster in projection: its velocity distribution is Gaussian $\left(\chi^2 = 0.09\right)$ but a rich neighbour (richness ratio 1:1.6) lies within 2Mpc. On the third line, the C4 cluster 0126 is an example of minor multimodal clusters with a Gaussian velocity distribution $\left(\chi^2 = 0.18\right)$ and a neighbour with richness ratio of 1:6 within 2Mpc. The C4 cluster 0017 (bottom panels) is an irregular unimodal cluster with a Gaussian velocity distribution $\left(\chi^2 = 0.09\right)$, without neighbour and with high ellipticity ($\epsilon = 0.51$).

5 Conclusion

This work presents a new optical approach to classify galaxy clusters using both galaxy velocity distribution and galaxy projected distribution. A fraction of 65% of non regular clusters is found, which is in good agreement with previous studies: at least 40% (Geller & Beers 1982; Kolokotronis et al. 2001) and up to 70% of clusters present substructures in the local universe (Dressler & Shectman 1988; Girardi et al. 1997; Einasto et al. 2012).

This classification provides a statistical sample of clusters to study environment effects on galaxies according to their cluster dynamical state. It will also be used as a reference for a similar study based on photometric redshifts and/or at higher redshifts (CFHT-LS, EUCLID, DES, etc.).

References

Abazajian, K., Adelman-McCarthy, J. K., Agüeros, M. A., et al. 2004, AJ, 128, 502

Ashman, K. M., Bird, C. M., & Zepf, S. E. 1994, AJ, 108, 2348

Bautz, L. P. & Morgan, W. W. 1970, ApJ, 162, L149

Beers, T. C., Flynn, K., & Gebhardt, K. 1990, AJ, 100, 32

Bertin, E. & Arnouts, S. 1996, A&AS, 117, 393

Buote, D. A. & Tsai, J. C. 1996, ApJ, 458, 27

Dressler, A. & Shectman, S. A. 1988, AJ, 95, 985

Einasto, M., Vennik, J., Nurmi, P., et al. 2012, A&A, 540, A123

Ferrari, C., Benoist, C., Maurogordato, S., Cappi, A., & Slezak, E. 2005, A&A, 430, 19

Flin, P. & Krywult, J. 2006, A&A, 450, 9

Geller, M. J. & Beers, T. C. 1982, PASP, 94, 421

Girardi, M., Escalera, E., Fadda, D., et al. 1997, ApJ, 482, 41

Jones, C. & Forman, W. 1999, ApJ, 511, 65

Kolokotronis, V., Basilakos, S., Plionis, M., & Georgantopoulos, I. 2001, MNRAS, 320, 49

McLachlan, G. & Peel, D. 1999, Journal of Statistical Software, 4, 1

Melott, A. L., Chambers, S. W., & Miller, C. J. 2001, ApJ, 559, L75

Miller, C. J., Nichol, R. C., Reichart, D., et al. 2005, AJ, 130, 968

Mohr, J. J., Fabricant, D. G., & Geller, M. J. 1993, ApJ, 413, 492

Plionis, M. 2002, ApJ, 572, L67

Ramella, M., Biviano, A., Pisani, A., et al. 2007, A&A, 470, 39

Rood, H. J. & Sastry, G. N. 1971, PASP, 83, 313

Schuecker, P., Böhringer, H., Reiprich, T. H., & Feretti, L. 2001, A&A, 378, 408

York, D. G., Adelman, J., Anderson, Jr., J. E., et al. 2000, AJ, 120, 1579

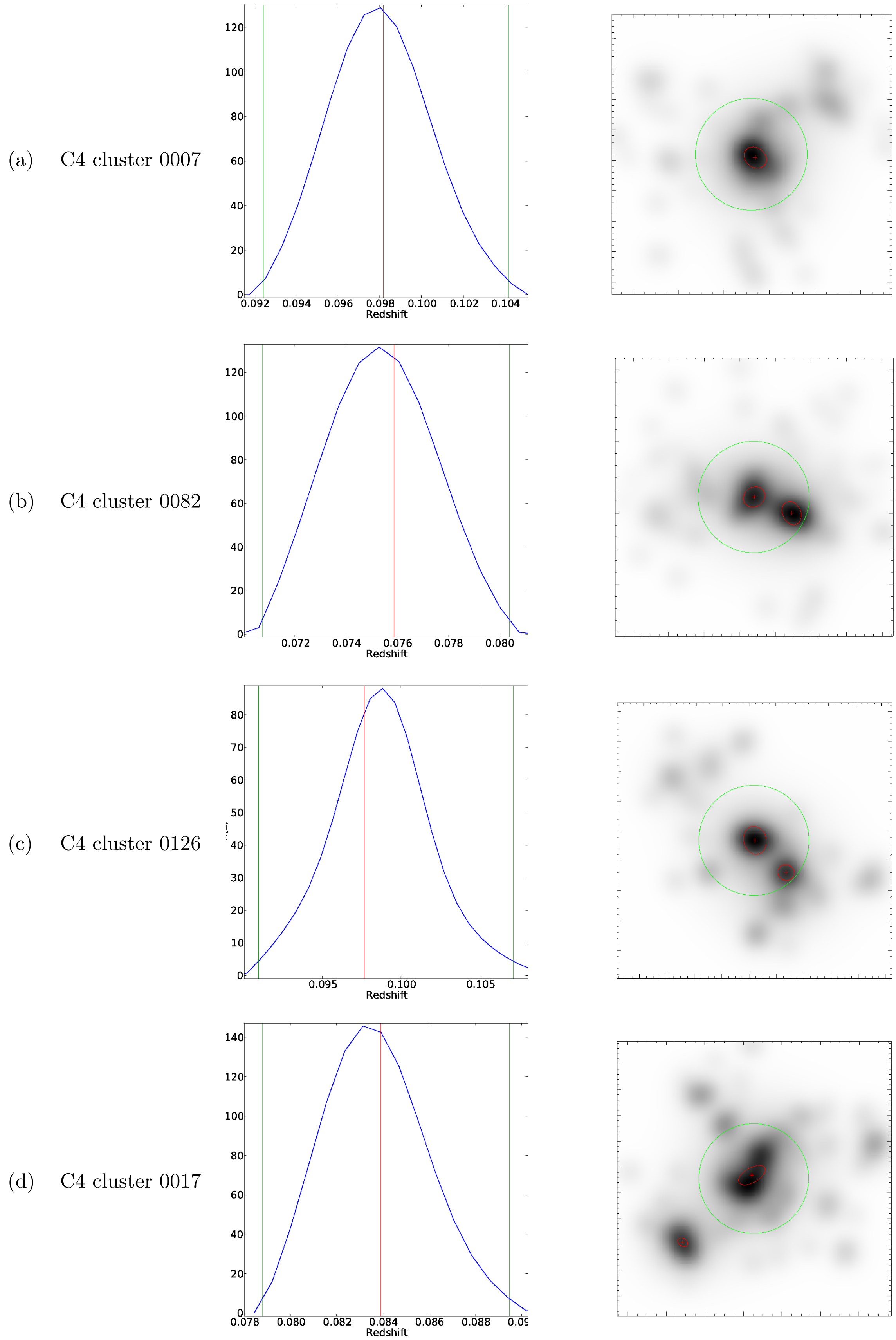

Fig. 1. Examples of the four cluster morphologies. **Left panels**: cluster redshift distribution function (RDF) with C4 cluster redshift (red) and the redshift interval used to build the cluster density map (green). **Right panels**: density maps with detected overdensities indicated by the red ellipses and the green circle represents the distance of 2Mpc from the main cluster (at the center). Panels (a): example of a regular cluster. Panels (b): example of a major bimodal cluster. Panels (c): example of a minor multimodal cluster. Panels (d): example of an irregular unimodal cluster.